Supporting information for

Two groups of copperⅡ pyridine-triazole complex with "open or close" pepper rings and their in-vitro antitumor activities

ZhaoGuo Hong[a], Chu Zheng[a], Bi Luo[a], Xin You[a], HeDong Bian[b], Hong Liang[a], FengZhen Chen*[a] and FuPing Huang*[a]

[a] State Key Laboratory for Chemistry and Molecular Engineering of Medicinal Resources, School of Chemistry and Pharmacy, Guangxi Normal University, Guilin 541004, PR China

[b] School of Chemistry and Chemical Engineering, Guangxi University for Nationalities, Key Laboratory of Chemistry and Engineering of Forest Products, Nanning 530008, PR China

Table S1 Crystallographic data and structure refinement parameters for complexes **C1-C6**

Complex	**C1**	**C2**	**C3**
Empirical formula	$C_{15}H_{14}Cl_2CuN_4O_2$ ·0.25(H_2O)	$C_{30}H_{28}ClCuN_8O_8$· ClO_4	$C_{30}H_{26}Cu_2N_{12}O_{14}$· C_2H_3N
Formula weight (*M*)	421.24	827.04	946.76
Crystal system	Monoclinic	Monoclinic	Monoclinic
Space group	$P2_1/n$	$P2_1/n$	$P2_1/n$
a (Å)	10.2362(5)	8.6128(4)	13.6199(3)
b (Å)	17.5970(6)	18.2300(7)	12.0853(3)
c (Å)	10.3334(10)	21.5956(9)	23.0230(5)
α (°)	90.00	90.00	90.00
β (°)	109.474(8)	94.990 (4)	98.247(2)
γ (°)	90.00	90.00	90.00
V/(Å^3)	1754.8 (2)	3377.9 (2)	3750.40(15)
Z	4	4	4
D_c(Mg cm^{-3})	1.593	1.626	1.677
F(000)	852	1692	1928
θ range for data collection (°)	4.0-26.3	3.7-26.5	3.7-27.8
Reflections collected/unique	10804 /3216 [*R*(int) =0.038]	21681/6888 [*R*(int) =0.038]	27321/7617 [*R*(int) =0.033]
Goodness-of-fit on F^2	1.05	1.05	1.02

Final *R* indices [$I > 2\sigma(I)$]	$R_1 = 0.0541$ $\omega R_2 = 0.1551$	$R_1 = 0.0639$ $\omega R_2 = 0.1787$	$R_1 = 0.0584$ $\omega R_2 = 0.0997$
R indices (all data)	$R_1 = 0.0766$ $\omega R_2 = 0.1724$	$R_1 = 0.2089$ $\omega R_2 = 0.0895$	$R_1 = 0.0402$ $\omega R_2 = 0.1094$

Complex	**C4**	**C5**	**C6**
Empirical formula	$C_{16}H_{16}Cl_2CuN_4O_3S \cdot C_2H_6OS$	$C_{14}H_{10}CuN_4O_6S \cdot CH_4O$	$C_{28}H_{18}Cu_2N_{10}O_{10} \cdot CH_3CH_2OH$
Formula weight (*M*)	556.99	457.90	827.69
Crystal system	Monoclinic	Monoclinic	Monoclinic
Space group	$P2_1/c$	$P2_1$	$P2_1/c$
a (Å)	9.6197(12)	10.616(3)	11.0710(6)
b (Å)	22.809(3)	7.3808(18)	33.288(2)
c (Å)	13.0632(12)	10.876(3)	26.7627(11)
α (°)	90.00	90.00	90.00
β (°)	127.446(6)	100.629(4)	100.081(5)
γ (°)	90.00	90.00	90.00
V/(Å^3)	2275.6(5)	837.6(4)	9710.6(9)
Z	4	2	12
D_c(Mg cm^{-3})	1.626	1.816	1.698
F(000)	1140	466	5039
θ range for data collection (°)	2.2-26.3	2.5-26.3	3.7-21.4
Reflections collected/unique	26984/4110 [*R*(int) =0.032]	10173/3028 [*R*(int) =0.032]	109498/8449 [*R*(int) =0.148]
Goodness-of-fit on F^2	1.10	1.05	1.02
Final *R* indices [$I > 2\sigma(I)$]	$R_1 = 0.0279$ $\omega R_2 = 0.0818$	$R_1 = 0.0284$ $\omega R_2 = 0.060$	$R_1 = 0.1977$ $\omega R_2 = 0.2169$
R indices (all data)	$R_1 = 0.0325$ $\omega R_2 = 0.0842$	$R_1 = 0.0363$ $\omega R_2 = 0.0622$	$R_1 = 0.1073$ $\omega R_2 = 0.2663$

Table S2 Selected bond lengths (Å) and angles (º) for complexes **C1-C6**

C1			
Cu1—Cl2	2.2971 (14)	Cu1—Cl1	2.2399 (14)
Cu1—N1	2.075 (3)	Cu1—N3	1.963 (4)
Cl1—Cu1—Cl2	97.54 (6)	N1—Cu1—Cl2	148.82 (13)
N1—Cu1—Cl1	93.45 (11)	N3—Cu1—Cl2	94.07 (12)
N3—Cu1—Cl1	167.66 (13)	N3—Cu1—N1	78.57 (15)
C2			
Cu1—N5	2.021 (3)	Cu1—N3	1.968 (3)
Cu1—N1	2.025 (3)	Cu1—N7	1.959 (3)
Cu1—O5	2.372 (4)		
N5—Cu1—N1	176.30 (15)	N5—Cu1—O5	95.76 (15)
N3—Cu1—N5	98.98 (14)	N3—Cu1—N1	80.97 (13)
N3—Cu1—O5	97.69 (15)	N1—Cu1—O5	87.91 (14)
N7—Cu1—N5	81.25 (14)	N7—Cu1—N3	166.01 (15)
N7—Cu1—N1	97.89 (13)	N7—Cu1—O5	96.19 (15)
C3			
Cu1—N9	1.977 (2)	Cu1—N3	1.979 (2)
Cu1—N1	2.040 (3)	Cu1—O9	1.964 (2)
Cu2—N8	1.973 (2)	Cu2—N6	2.018 (3)
Cu2—N4	1.957 (3)	Cu2—O13	2.436 (3)
Cu2—O12	1.978 (2)		
N9—Cu1—N3	97.58 (10)	N9—Cu1—N1	177.94 (10)
N3—Cu1—N1	80.72 (10)	O9—Cu1—N9	94.18 (9)
O9—Cu1—N3	164.92 (10)	O9—Cu1—N1	87.31 (10)
N8—Cu2—N6	81.46 (10)	N8—Cu2—O13	110.83 (11)
N8—Cu2—O12	165.03 (11)	N6—Cu2—O13	97.96 (11)
N4—Cu2—N8	97.57 (10)	N4—Cu2—N6	166.56 (11)
N4—Cu2—O13	94.92 (12)	N4—Cu2—O12	92.23 (10)
O12—Cu2—N6	91.59 (10)	O12—Cu2—O13	56.78 (11)
C4			
Cu1—Cl1	2.3357 (7)	Cu1—Cl2	2.3969 (7)
Cu1—O3	1.9715 (15)	Cu1—N1	2.1231 (16)
Cu1—N3	2.0207 (16)		
Cl1—Cu1—Cl2	118.99 (2)	O3—Cu1—Cl1	91.19 (5)
O3—Cu1—Cl2	91.35 (6)	O3—Cu1—N1	86.62 (6)
O3—Cu1—N3	166.98 (6)	N1—Cu1—Cl1	126.98 (5)
N1—Cu1—Cl2	114.02 (5)	N3—Cu1—Cl1	97.36 (5)
N3—Cu1—Cl2	93.05 (5)	N3—Cu1—N1	80.39 (6)
C5			
Cu1—N1	1.997 (2)	Cu1—N2	2.009 (2)
Cu1—O3	1.9995 (17)	Cu1—O4	1.9720 (18)
O3—Cu1—N2	172.99 (11)	O4—Cu1—N1	169.56 (8)

O4—Cu1—N2	106.97 (8)	O4—Cu1—O3	71.44 (7)
		C6	
Cu1—O8	1.969 (7)	Cu3—N12	1.956 (7)
Cu1—O9	2.532 (9)	Cu3—N18	1.954 (8)
Cu1—N1	2.030 (9)	Cu3—N20	2.566 (9)
Cu1—N2	1.941 (8)	Cu4—O15	1.973 (7)
Cu1—N8	1.963 (8)	Cu4—O17	2.547 (9)
Cu1—N10	2.645 (11)	Cu4—N14	1.960 (8)
Cu2—O5	1.982 (7)	Cu4—N15	2.024 (9)
Cu2—O7	2.485 (9)	Cu4—N16	1.956 (8)
Cu2—N4	1.961 (8)	Cu4—N19	2.629 (10)
Cu2—N5	2.027 (8)	Cu5—O29	2.479 (9)
Cu2—N6	1.980 (8)	Cu5—O30	1.999 (7)
Cu2—N9	2.607 (12)	Cu5—N21	2.027 (9)
Cu3—O18	1.992 (6)	Cu5—N22	1.955 (8)
Cu3—O19	2.499 (8)	Cu5—N28	1.935 (9)
Cu3—N11	2.026 (8)	Cu5—N30	2.606 (10)
O8—Cu1—O9	54.8 (3)	O15—Cu4—O17	55.2 (3)
O8—Cu1—N1	91.2 (3)	O15—Cu4—N15	91.2 (3)
O8—Cu1—N10	28.2 (3)	O15—Cu4—N19	27.8 (3)
O9—Cu1—N10	26.7 (3)	O17—Cu4—N19	27.4 (3)
N1—Cu1—O9	96.9 (3)	N14—Cu4—O15	93.3 (3)
N1—Cu1—N10	96.4 (4)	N14—Cu4—O17	91.5 (3)
N2—Cu1—O8	165.0 (3)	N14—Cu4—N15	170.5 (4)
N2—Cu1—O9	112.8 (3)	N14—Cu4—N19	91.6 (3)
N2—Cu1—N1	81.6 (3)	N15—Cu4—O17	98.0 (3)
N2—Cu1—N8	96.7 (3)	N15—Cu4—N19	96.3 (4)
N2—Cu1—N10	139.3 (4)	N16—Cu4—O15	164.9 (3)
N8—Cu1—O8	92.8 (3)	N16—Cu4—O17	112.6 (3)
N8—Cu1—O9	93.9 (3)	N16—Cu4—N14	96.1 (3)
N8—Cu1—N1	168.8 (4)	N16—Cu4—N15	81.4 (3)
N8—Cu1—N10	92.0 (3)	N16—Cu4—N19	139.7 (4)
O5—Cu2—O7	56.1 (3)	O29—Cu5—N30	27.9 (3)
O5—Cu2—N5	90.8 (3)	O30—Cu5—O29	56.1 (3)
O5—Cu2—N9	28.1 (3)	O30—Cu5—N21	90.6 (3)
O7—Cu2—N9	28.1 (3)	O30—Cu5—N30	28.5 (3)
N4—Cu2—O5	94.3 (3)	N21—Cu5—O29	93.7 (3)
N4—Cu2—O7	99.7 (3)	N21—Cu5—N30	89.7 (3)
N4—Cu2—N5	170.5 (3)	N22—Cu5—O29	109.0 (3)
N4—Cu2—N6	95.7 (4)	N22—Cu5—O30	162.8 (3)
N4—Cu2—N9	99.7 (3)	N22—Cu5—N21	81.2 (3)
N5—Cu2—O7	89.8 (3)	N22—Cu5—N30	135.5 (4)
N5—Cu2—N9	88.5 (4)	N28—Cu5—O29	96.5 (3)
N6—Cu2—O5	163.2 (3)	N28—Cu5—O30	94.1 (3)

N6—Cu2—O7	108.7 (3)	N28—Cu5—N21	169.7 (4)
N6—Cu2—N5	81.3 (4)	N28—Cu5—N22	96.4 (4)
N6—Cu2—N9	136.1 (4)	N28—Cu5—N30	98.8 (3)
O18—Cu3—O19	56.7 (3)	O25—Cu6—O27	55.4 (3)
O18—Cu3—N11	90.4 (3)	O25—Cu6—N25	91.6 (4)
O18—Cu3—N20	29.3 (3)	O25—Cu6—N26	165.0 (4)
O19—Cu3—N20	27.6 (3)	O25—Cu6—N29	27.8 (3)
N11—Cu3—O19	90.0 (3)	O27—Cu6—N29	27.6 (3)
N11—Cu3—N20	87.4 (3)	N24—Cu6—O25	92.9 (3)
N12—Cu3—O18	163.5 (3)	N24—Cu6—O27	93.6 (3)
N12—Cu3—O19	108.6 (3)	N24—Cu6—N25	171.0 (4)
N12—Cu3—N11	81.7 (3)	N24—Cu6—N26	95.5 (4)
N12—Cu3—N20	135.1 (4)	N24—Cu6—N29	92.8 (3)
N18—Cu3—O18	94.9 (3)	N25—Cu6—O27	95.4 (3)
N18—Cu3—O19	101.4 (3)	N25—Cu6—N29	94.9 (4)
N18—Cu3—N11	168.5 (3)	N26—Cu6—O27	111.6 (3)
N18—Cu3—N12	95.6 (3)	N26—Cu6—N25	81.8 (4)
N18—Cu3—N20	102.2 (3)	N26—Cu6—N29	139.0 (3)

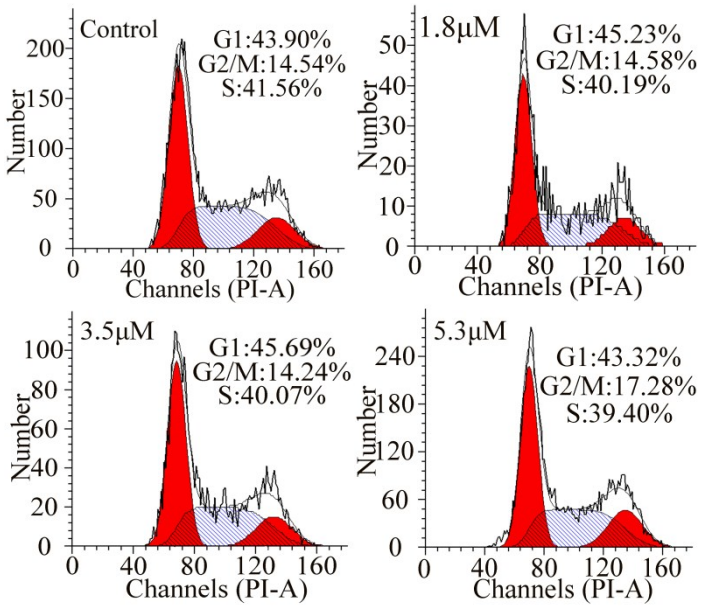

Figure S1: Analysis of cell cycle arrest by flow cytometry in T24 cells after 24 h treatment with C1.

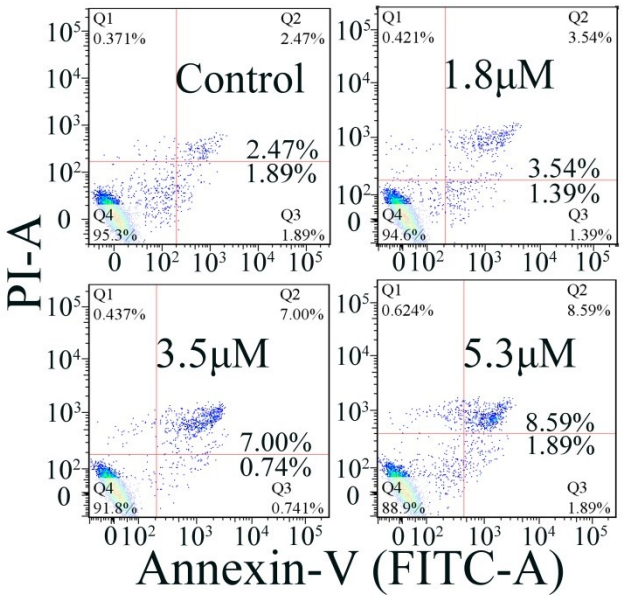

Figure S2: Apoptosis of T24 cells induced by C1, detected using flow cytometry after 24 h.

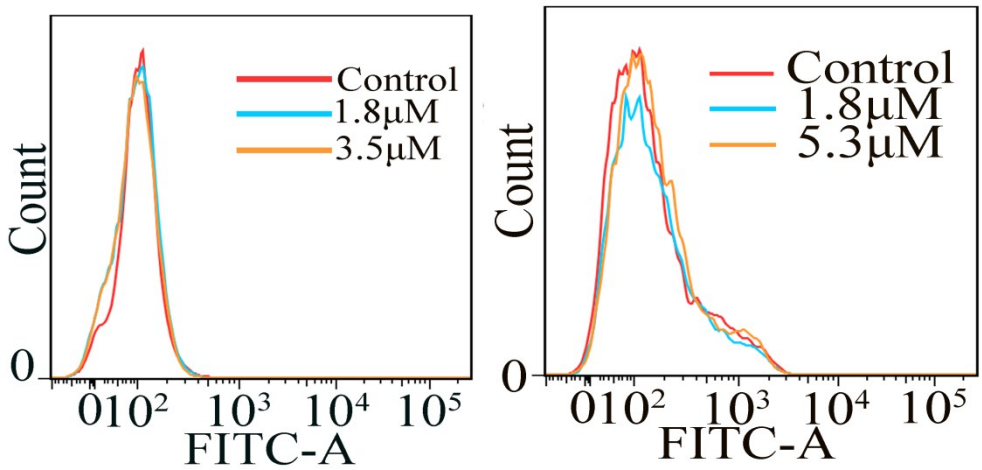

Figure S3: Analysis of reactive oxygen species level and calcium release by flow cytometry in T24 cells after 24 h treatment with C1.

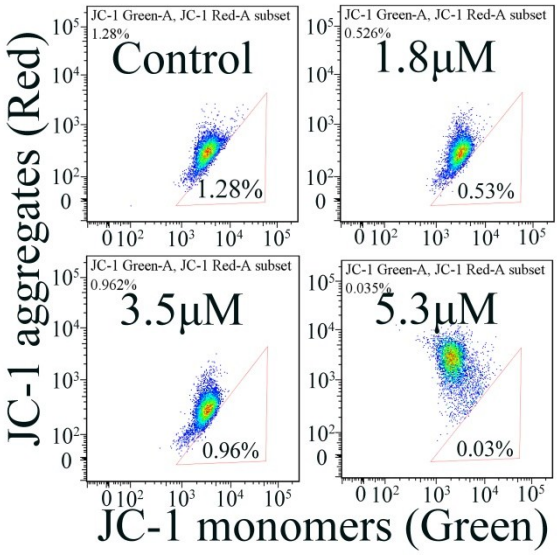

Figure S4: Measurement of mitochondrial membrane potential by flow cytometry in T-24 cells after 24 h treatment with C1.

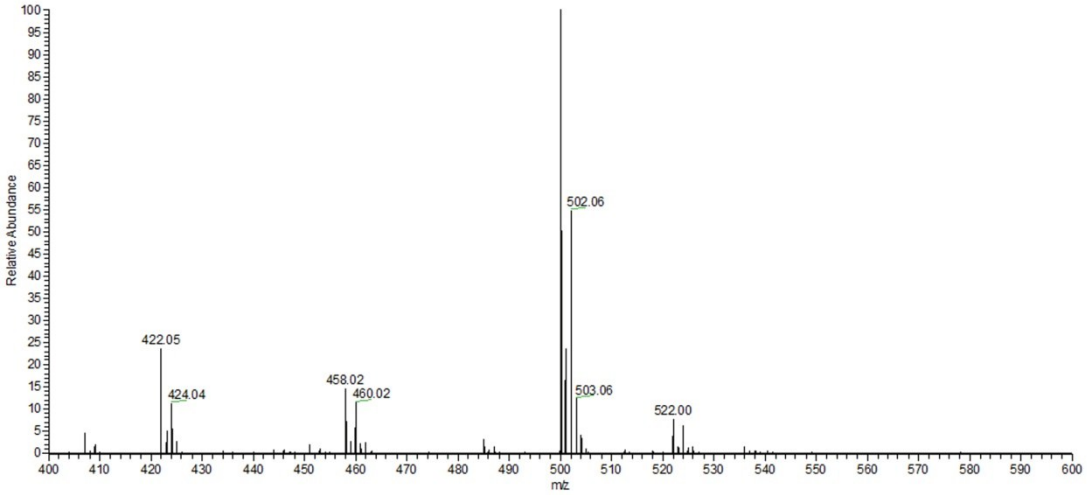

Figure S5: Mass Spectrum of C1

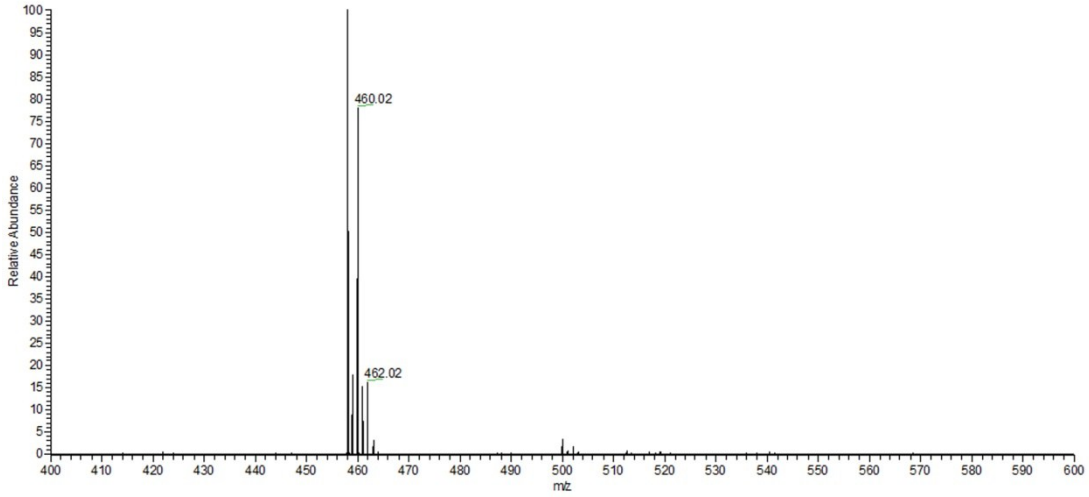

Figure S6: Mass Spectrum of C2

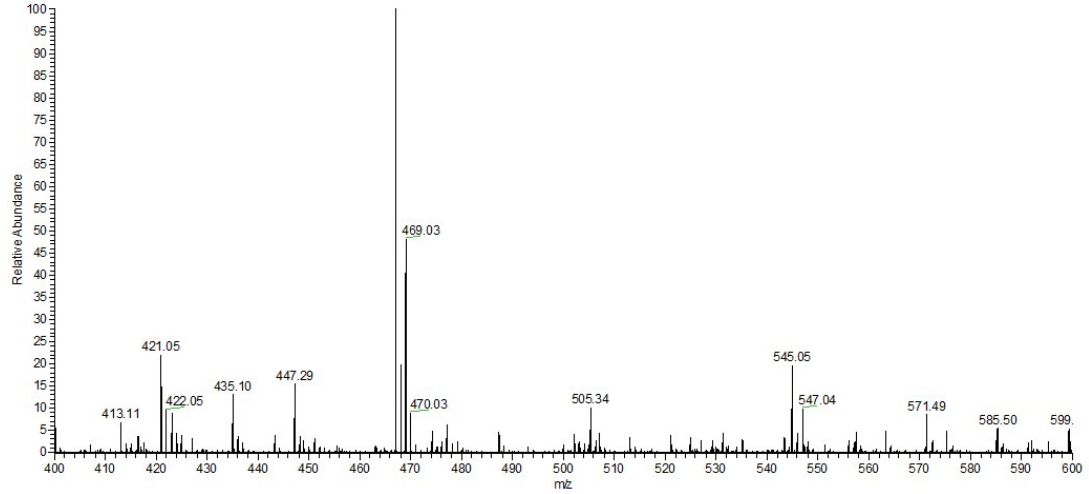

Figure S7: Mass Spectrum of C3

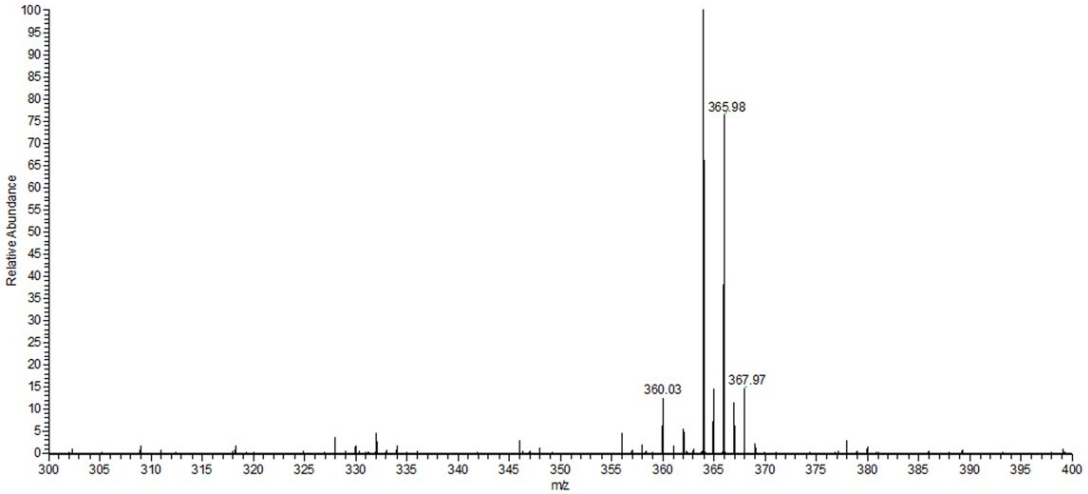

Figure S8: Mass Spectrum of C4

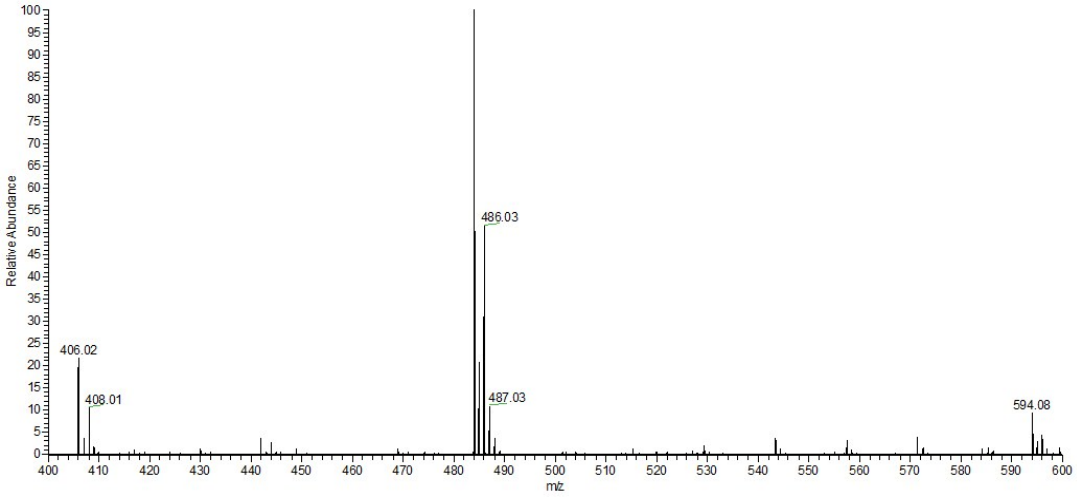

Figure S9: Mass Spectrum of C5

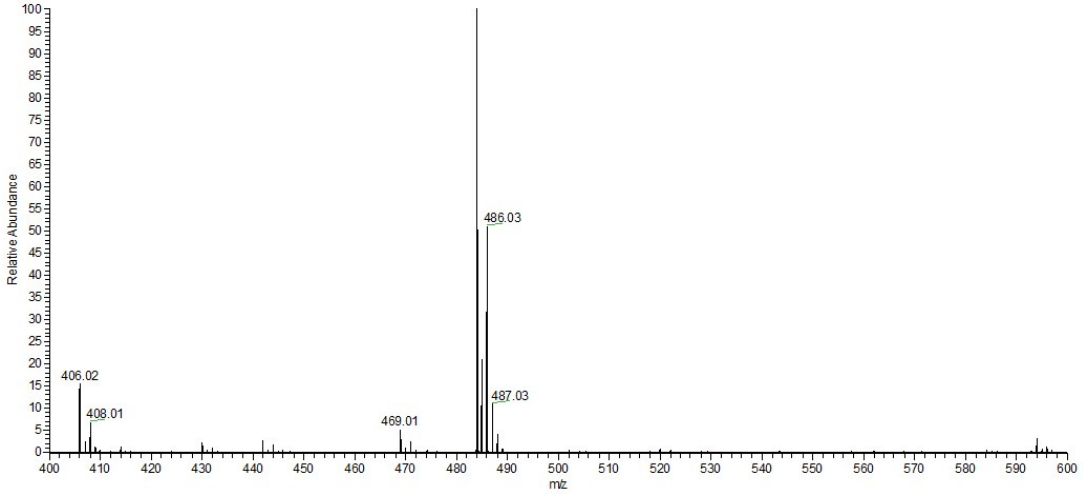

Figure S10: Mass Spectrum of C6

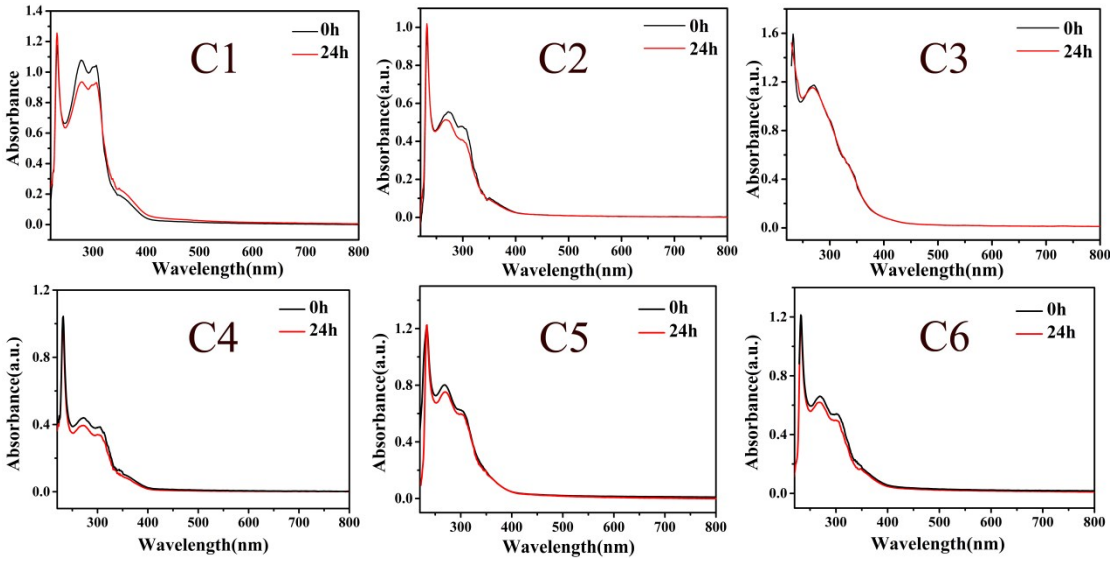

Figure S11: UV-Vis Spectrum of C1-C6

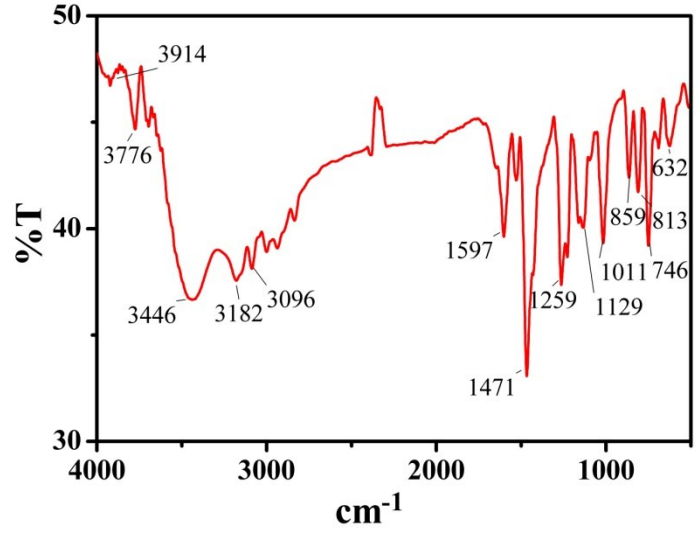

Figure S12: Infrared spectrum of L^1

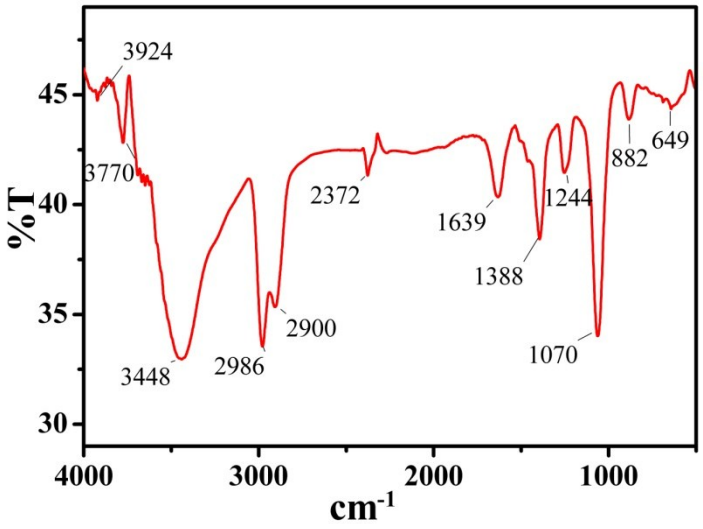

Figure S13: Infrared spectrum of L^2

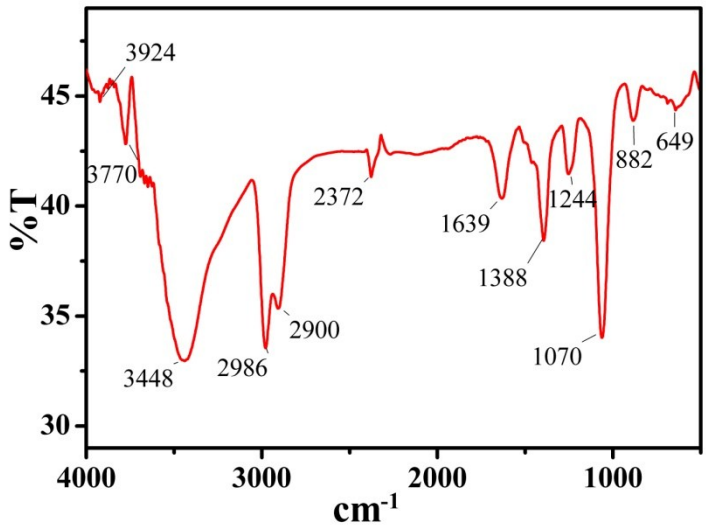

Figure S14: Infrared spectrum of C1

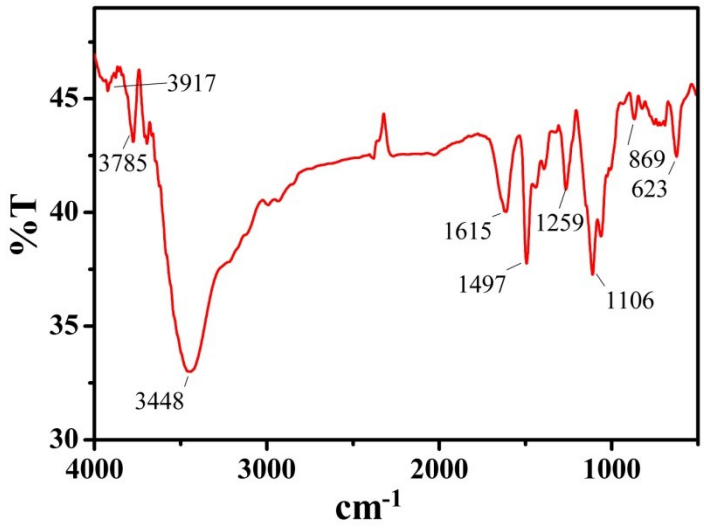

Figure S15: Infrared spectrum of C2

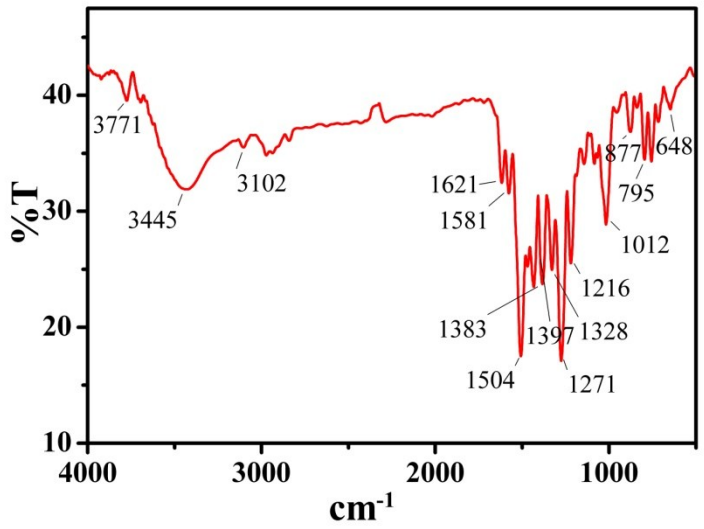

Figure S16: Infrared spectrum of C3

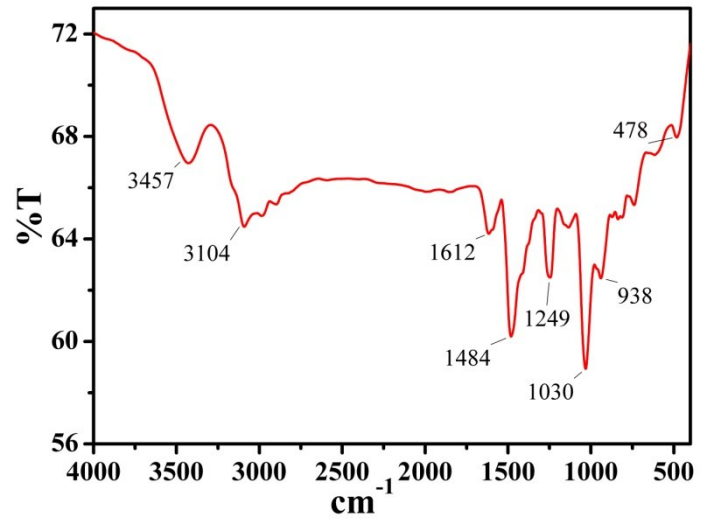

Figure S17: Infrared spectrum of C4

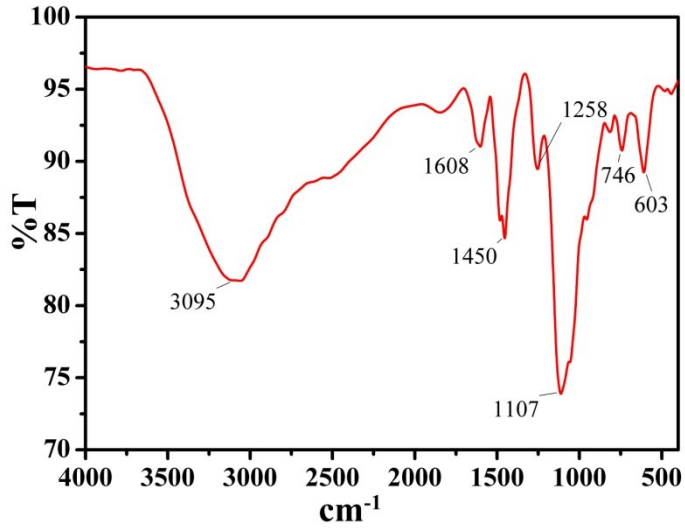

Figure S18: Infrared spectrum of C5

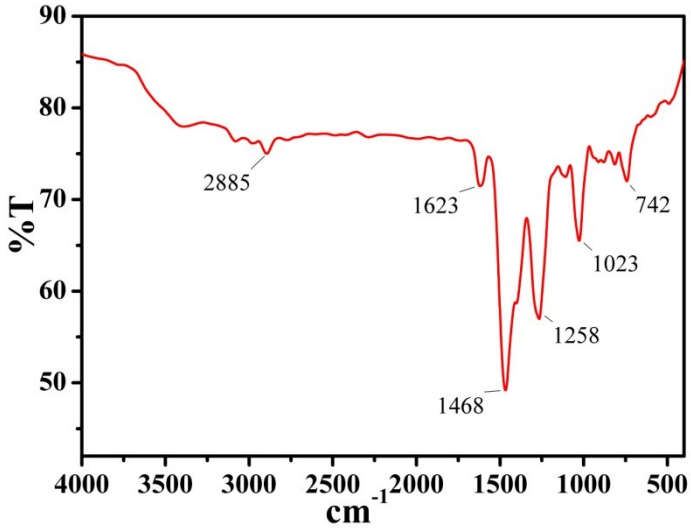

Figure S19: Infrared spectrum of C6

Experimental detail

Synthesis of L^1 and L^2

The synthetic route of the ligand **L^1** and **L^2** is shown in Fig.S20. Briefly, To a solution of sodium alkoxide solution was added 2,3-dimethoxybenzonitrile(20 mmol, 2.94 g). The reaction mixture was stirred for 2 h at room temperature. Then, to the resulting solution, adding picolinohydrazide (20 mmol, 2.74 g) and refluxed for 24 h at 85 °C. After cooling, the products was washing with water, collect solid, then using acetic acid to adjust the pH to neutral, obtaining a yellow solid product. Recrystallization gave pale yellow powder (yield: 65 %). Elemental analysis: calculated (%) for **L^1,** $C_{15}H_{14}N_4O_2$ (282.11): C, 63.80; H, 4.96; N, 19.85. Found (%): C, 61.93; H, 3.75; N, 21.29. ESI-MS: m/z=289.07 [**L^1**-Na]$^+$. FT-IR [KBr phase, cm^{-1}]: 3914 w, 3776 m, 3446 m, 3182 m, 3096 m, 1597 s, 1471 s, 1259 s, 1129 m, 1011 s, 859 m, 813 m, 746 s, 632 m. The same synthetic procedure as that for **L^1** except that 2,3-dimethoxybenzonitrile was replaced by piperonylonitrile, and yellow block crystals were obtained in 70 % yield. Elemental analysis: calculated (%) for **L^2**, $C_{14}H_{10}N_4O_2$ (266.26): C, 63.10; H, 3.76; N, 21.03. Found (%): C, 63.32; H, 3.58; N, 21.94. ESI-MS(+): m/z=289.07 [**L^2**-Na]$^+$. FT-IR [KBr phase, cm^{-1}]: 3431 w, 2899 w,

1595 w, 1462 s, 1411 s, 1246 s, 1133 w, 1039 s, 935 s, 867 s, 740 m, 561 w.

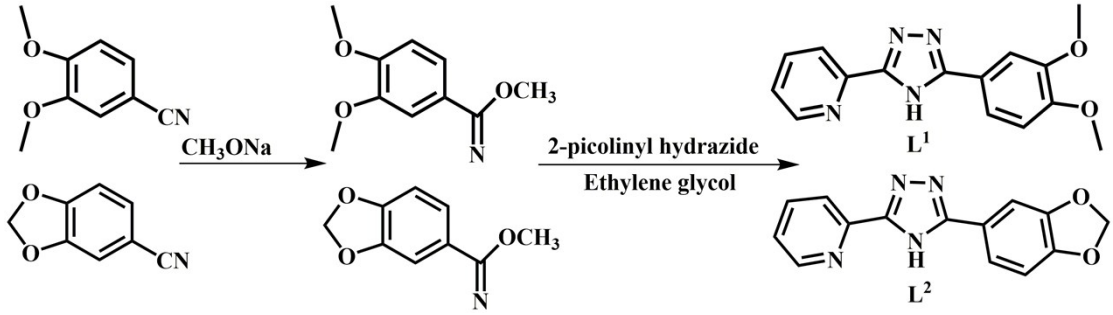

Figure S20: Synthetic route of L^1 and L^2

Synthesis of C1-C6

$[Cu(L^1)Cl_2]\cdot 0.25H_2O$ (C1) A mixture solution (10 mL) containing **L^1** (0.3 mmol, 0.08463 g), $CuCl_2\cdot 2H_2O$ (0.3 mmol, 0.0511 g) and methanol (10 mL) in a Teflon-lined stainless steel vessel (23 mL) was heated at 80 °C for 48 h and then cooled to room temperature at 5 °C/h. Green block crystals were obtained in 65 % yield. Elemental analysis: calculated (%) for $C_{15}H_{14.5}Cl_2CuN_4O_{2.25}$ (421.24): C, 42.73; H, 3.44; N, 13.29. Found (%): C, 40.62; H, 2.79; N, 14.51. ESI-MS(+): m/z=500.06 $[Cu(L^1)]^+\cdot$2DMSO. FT-IR [KBr, cm^{-1}]: 3924 w, 3770 m, 3448 s, 2986 s, 2900 w, 2372 w, 1639 m, 1388 s, 124 4m, 1070 s, 882 w, 649 w.

$[Cu(L^1)_2(ClO_4)]\cdot ClO_4$ (C2) C2 was obtained by a similar method as described for **C1** using $Cu(ClO_4)_2\cdot 6H_2O$ (0.3 mmol, 0.1111 g) in place of $CuCl_2\cdot 2H_2O$. Green block crystals were obtained in 60 % yield. Elemental analysis: calculated (%) for $C_{30}H_{28}Cl_2CuN_8O_{12}$ (827.04): C, 43.53; H, 3.38; N, 13.54. Found (%): C, 42.03; H, 3.12; N, 15.13. ESI-MS(+): m/z=458.02 $[Cu(L^1)]^+\cdot$MeOH$\cdot$2CH_3CN. FT-IR [KBr, cm^{-1}]: 3917 w, 3785 m, 3448 s, 1615 s, 1497 s, 1259 s, 1106 s, 869 w, 623 m.

$[Cu_2(L^{1'})_2(NO_3)_2]\cdot CH_3CN$ (C3) C3 was obtained by a similar method as described for **C1** using $Cu(NO_3)_2\cdot 3H_2O$ (0.3 mmol, 0.0725 g) in place of $CuCl_2\cdot 2H_2O$. Surprisingly, this ligand was nitrified in the reaction process. Green block crystals were obtained in 65 % yield. Elemental analysis: calculated (%) for $C_{32}H_{29}Cu_2N_{13}O_{14}$ (946.76): C, 40.56; H, 3.06; N, 19.22. Found (%): C, 38.98; H, 3.32; N, 21.12. ESI-MS(+): m/z=467.03 $[Cu(L^1)]^+\cdot$2DMSO. FT-IR [KBr, cm^{-1}]: 3771 w, 3445 m, 3102 w, 2968 w, 1621 m, 1581 m, 1504 s, 1397 s, 1383 m, 1328 m, 1271 s, 1216 s, 1012s, 877 w, 795 m, 648 w.

$[Cu(L^2)(DMSO)Cl_2]\cdot$DMSO (C4) A mixture solution (11 mL) containing **L^2** (0.3 mmol, 0.0798 g), $CuCl_2\cdot 2H_2O$ (0.3 mmol, 0.0511 g), ethanol (10 mL) and DMSO (1 mL) in a Teflon-lined stainless steel vessel (23 mL) was heated at 80 °C for 48 h and then cooled to room temperature at 5 °C/h. Yellow block crystals were obtained in 60 % yield. Elemental analysis: calculated (%) for $C_{18}H_{22}Cl_2CuN_4O_4S_2$ (556.99): C, 38.78; H, 3.95; N, 10.05. Found (%): C, 38.65; H, 3.82; N, 10.12. ESI-MS(+): m/z=363.98 $[Cu(L^2)]^+\cdot 2H_2O$. FT-IR [KBr, cm^{-1}]: 3426 w, 3097 w, 1609 w, 1477 s, 1419 m, 1252 s, 1148 w, 1035 s, 985 w, 932 w, 736 w, 473 w.

$[Cu(L^2)SO_4]\cdot CH_3OH$ (C5) A mixture solution (10 mL) containing **L^2** (0.3 mmol, 0.0798 g), $CuSO_4\cdot 5H_2O$ (0.3 mmol, 0.0749 g) and methanol (10 mL) in a Teflon-lined stainless steel vessel (23 mL) was heated at 80 °C for 48 h and then cooled to room temperature at 5 °C/h. Green block crystals were obtained in 70 % yield. Elemental analysis: calculated (%) for $C_{14}H_{10}CuN_4O_6S\cdot CH_4O$ (457.90): C, 39.31; H, 3.06; N, 12.23. Found (%): C, 39.42; H, 3.15; N, 12.34. ESI-MS(+): m/z=484.03

$[Cu(L^2)]^+$•2DMSO. FT-IR [KBr phase, cm^{-1}]: 3057 m, 2904 w, 1614 w, 1469 m, 1437 m, 1260 m, 1124 s, 1036 s, 973 m, 930 m, 740 m, 621 m, 427 w.

$[Cu_2(L^2)_2(NO_3)_2]$•C_2H_5OH (C6). A mixture solution (10 mL) containing **L^2** (0.3 mmol, 0.0798 g), $Cu(NO_3)_2 \cdot 3H_2O$ (0.3 mmol, 0.0725 g) and ethanol(10 mL) in a Teflon-lined stainless steel vessel (23 mL) was heated at 80 °C for 48 h and then cooled to room temperature at 5 °C/h. Green flake crystals were obtained in 50 % yield. Elemental analysis: calculated (%) for $C_{28}H_{18}Cu_2N_{10}O_{10}$•$C_2H_5OH$ (827.69): C, 43.49; H, 2.90; N, 16.91. Found (%): C, 43.56; H, 2.82; N, 17.84. ESI-MS(+): m/z=484.03 $[Cu(L^2)]^+$•2DMSO. FT-IR [KBr phase, cm^{-1}]: 3396 w, 2896 w, 1616 m, 1473 s, 1386 m, 1284 s, 1244 s, 1115 w, 1036 s, 932 w, 887 w, 753 m, 588 w.

Cellular studies

T24 cells were plated in 10-mm culture dishes at a density of 106 cells per mL and incubated in a 5% CO_2 and 37 ℃ incubator for 24 h, after the addition of 3.5 μM C1, C4 and further incubation for 24 h. After the treatment, the complex-containing medium was removed and cells were washed with ice-cold PBS three times and harvested in a tube. Then, the cytomembrane, nuclei, mitochondria, and remaining cytoplasm protein were extracted with the corresponding kit (Beyotime Biological Co., Ltd. Shanghai, china), respectively, and quantified by ICP-MS analysis (The copper content of the control group has been deducted).

MTT assay

In-vitro cytotoxicity activities of all complexes were measured by a colorimetric MTT assay. All complexes were dissolved in DMSO and further diluted to the required concentrations with cell culture medium. Briefly, cells (10^4 cells/well) were cultured in 96-well plates and controlled in an environment of 37 °C, 5 % CO_2 for 24 h to allow cells attachment. Cells were treated with increasing concentrations (5, 10, 20, 50, 100 μM and 1.25, 2.5, 5, 10, 20 μM) of prepared complexes solution, and incubated for another 24 h. In addition, the corresponding blank control group was setting. 10 μL of MTT (5 mg/mL) solution was added to each well after incubation. After 1-4 h, the supernatant was aspirated, and the formed formazan crystal was dissolved by adding 100 μL of DMSO to each well. The absorbance of resulting solution was determined at 490 nm by enzyme labeling instrument. (Infinite M1000) IC_{50} values of each complex that induced 50 % inhibition of cell growth were calculated using SPSS software. Each test was repeated three times independently.

Cell cycle analysis

Flow cytometry was used to investigated the effect of T-24 cells on cell cycle after treated with various concentrations (0, 1.8, 3.5 and 5.3 μM) of **C4**. Briefly, cells suspension (10^5 cells/mL) was seeded in 70×70 mm culture dishes and incubated for 12 h, then treated with for 24 h. The harvested cells were fixed with 70 % ice-cold ethanol and stored in a refrigerator overnight at -20 °C. The cells were washed by PBS Buffer and resuspended in freshly-concentrated RNase (100 μg/mL) solution at 37 °C for 30 min in the dark. 25 μL of PI (50 μg/mL) was added to each sample, subsequently. After 10 min dark staining, the cell cycle distribution was measured by flow cytometry.

Annexin V-FITC/PI dual staining studies

T24 cells were seeded into 6-well plates at a density of 10^5 cells/well for 24 h at incubator (37 ℃, 5 % CO_2). Then, various concentrations (0, 1.8, 3.5 and 5.3 μM) of **C4** was added each well, incubated for another 24 h. The cells were harvested by trypsinization and resuspended in 500 μL of PBS binding buffer and incubated with 5 μL Annexin V-FITC (100 ng/mL) for 30 min in the dark at 37 °C, and then adding 5 μL propidium iodide (2 μg/mL). Lastly, the apoptosis results were detected by flow

cytometry.

Reactive oxygen species (ROS) level analysis

Cytometry method was used to detect ROS level in T-24 cells with a ROS assay kit. T-24 cells were treated with **C4** at different concentrations (i.e., 0, 1.8 and 3.5 μM). After 24 hours of incubation, cells were washed and harvested, subsequently. Next, cells were resuspended in reactive oxygen stain solution (DCFH-DA, 100 μM) at 37 °C for 20 min in the dark. The levels of intracellular ROS were investigated by flow cytometry. Data acquisition and analyses were carried out using FlowJo software.

Detection of calcium release

In the process of apoptosis, the increase of calcium ions concentration is closely related to the production and accumulation of ROS, interacting with reactive oxygen species. Calcium release level was detected by cytometry method with ancalcium assay kit. T-24 cells were treated with various concentrations (0, 1.8 and 3.5 μM) of **C4**. The cells were harvested by trypsinization after 24 h and resuspended in Fluo-3 AM staining solution (5 μM) at 37 °C for 20 min in the dark. And then, the cells were washed with DMEM medium to remove the extra Fluo-3 AM completely. The cells were suspended in DMEM medium (500 μL) and measured by flow cytometry.

Mitochondrial membrane potential (JC-1) studies

Mitochondrial membrane potential was detected by cytometry method with a JC-1 assay kit. T-24 cells were treated with various concentrations (0, 1.8, 3.5 and 5.3 μM) of **C4**. The cells were harvested by trypsinization after 24 h and resuspended in JC-1 staining solution (5X) at 37 °C for 20 min in the dark. Subsequently, the cells were washed three times by JC-1 (1X) Staining Buffer. The cells were measured by flow cytometry and date was analyzed by FlowJo software.

Caspases activation assay

The activity of Caspase-3/8/9 was determined by CaspGLOW™ Fluorescein Active Caspase-3/8/9 Staining Kit, respectively. T24 cells were treated with **C4** (1.8, 3.5, 5.3 μM) for 24 h. Cells were harvested and washed with PBS buffer solution, 300 μL PBS containing the staining solution (FITC-DEVD-FMK, FITC-IETD-FMK and FITC-LEHD-FMK, 1 μL, respectively) was added subsequently and incubated at 37 ℃ for 50 min. A flow cytometer was employed to detect Caspase-3/8/9 activity.

Western blot assay

Western blot analysis was performed with the concentration of **C4** (IC_{50}, $2\times IC_{50}$), the total protein of T24 cells were harvested in a RIPA buffer. Proteins were isolated from acrylamide gel (12%) and transferred to PVDF membrane, then incubated overnight at 4 ℃ with specific antibodies (APAF-1, Bax, Bcl-2, Cyto-c and β-Actin). After wash with TBST buffer (3×10 min), the PVDF membranes were incubated with secondary antibodies (1:2000) at room temperature for 1 h. After repeated washing, PVDF membranes were visualized using an enhanced ECL detection kit by chemiluminescence system (Kodak, Rochester, NY, USA).

Bovine Serum Albumin Binding Studies

UV-Vis Spectra

The BSA stock solution (1 μM) was prepared in advance in 50 mM phosphate buffer saline (PBS)/100 mM NaCl buffer at pH 7.4 and stored at 4 ℃. A BSA solution (3 mL, 1×10^{-6} M) was titrated by successive additions of the stock solutions of **C1**/**C4** (2.0×10^{-5} M) and the variations in the BSA absorption were recorded after each addition. The spectrum was scanned by a Cary 60 UV-visible spectrophotometer on the range of wavelength from 195 to 315 nm.

Fluorescence Spectra

Consistent with the above experiment, 3.0 mL of BSA solution (1.0×10^{-6} M) were added into quartz colorimetric utensil (1 cm), following, 1 μL stock solutions of **C1**/**C4** (2.0×10^{-3} M) were added gradually, the fluorescence intensity was recorded from 290 to 490 nm at 25 ℃, the excitation wavelength was 280 nm, the slit width of the excitation and emission was 5 nm, using fluorescence spectrophotometer (Cary Eclipse, Agilent).

Competitive Binding Experiments

UV-Vis Spectra

CT-DNA was gradually added into the mixed solution of 3.0 mL Tris-HCl-NaCl buffer (5 mM Tris-HCl and 50 mM NaCl, pH 7.35 at 25 ℃) and at a constant concentration of **C1**/**C4**. The absorption spectrum was recorded in the wavelength range of 250-500 nm.

Fluorescence Spectra

The solutions of GelRed and CT-DNA mixture ([GelRed]/[CT-DNA] = 1:10) were pre-incubated at -4 ℃. The variation of emission spectra was recorded by the addition of a 30 μL of **C1**/**C4** stock solutions step by step into the 3.0 mL mixture of GelRed and CT-DNA. The fluorescence quenching curves were recorded using fluorescence spectrophotometer. All samples were excited at 510 nm, and emission spectra were observed at about 600 nm.

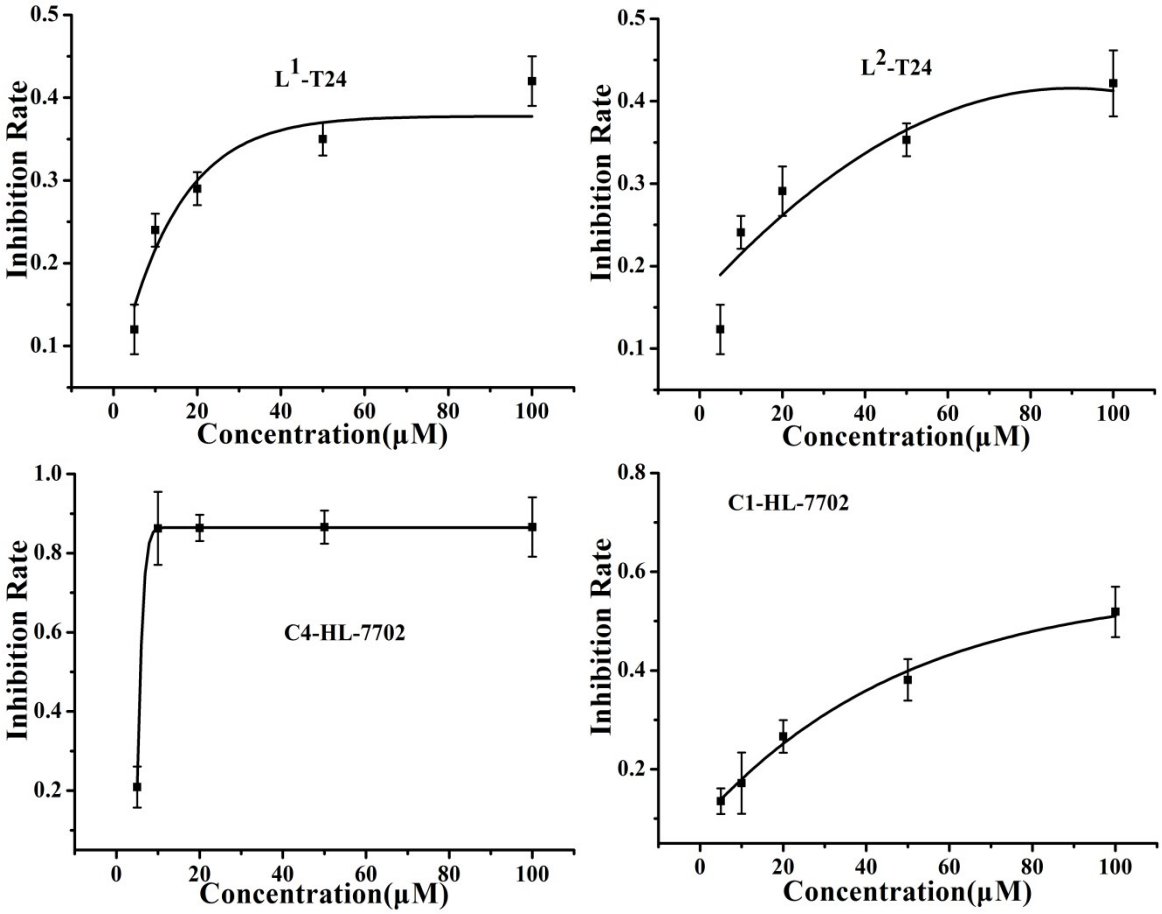

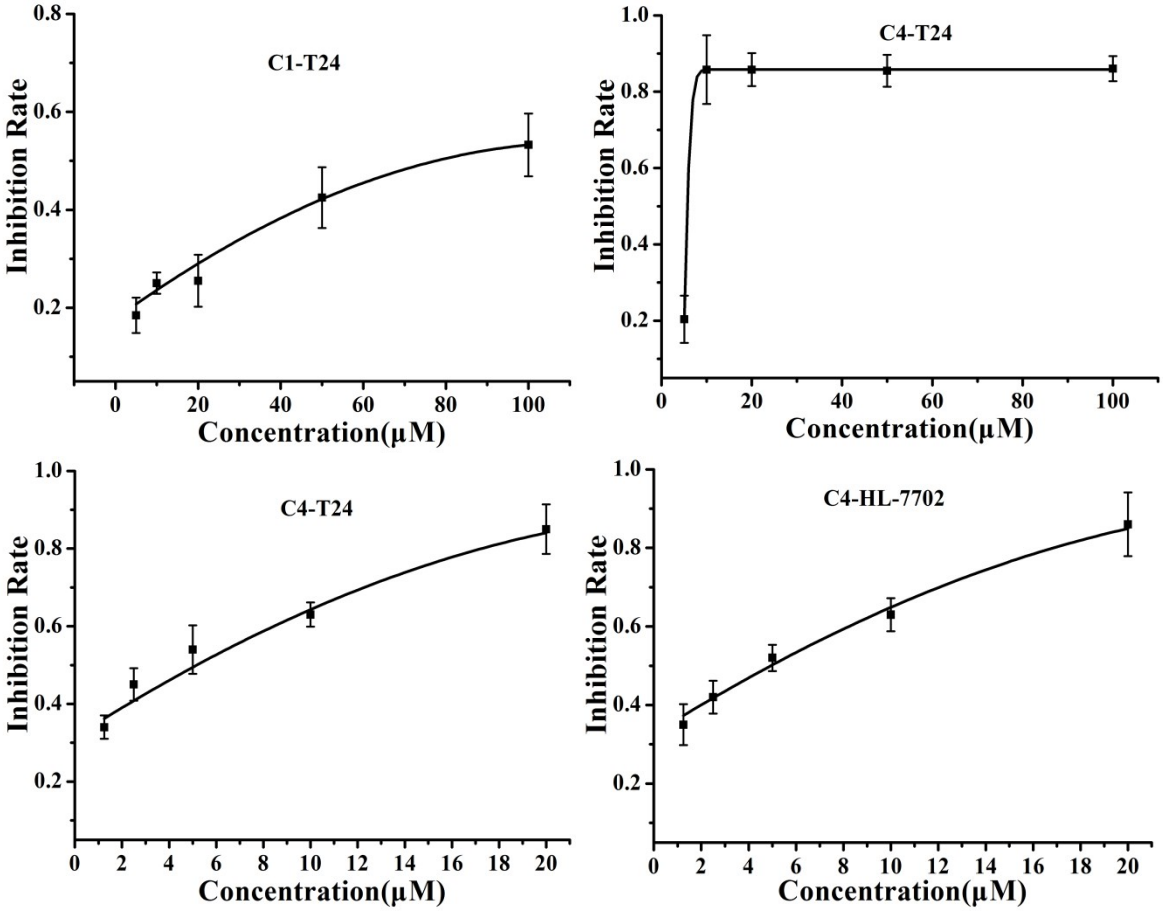

Figure S21: Parts of IC_{50} plots of compounds towards T24 and HL-7702 cells.

Abbreviations

T24 (human bladder cancer cell line)

Hep-G2 (human hepatocellular carcinoma cell line)

MGC-803 (human gastric cancer cell line)

HeLa (human cervical cancer cell line)

A549 (non-small cell lung cancer cell line)

NCI-H460 (large cell lung cancer cell line)

HL-7702 (human normal liver cell line)